JOURNAL OF COMPUTATIONAL PHYSICS 10, 185–201 (1972)

Numerical Method for Describing Turbulent, Compressible, Subsonic Separated Jet Flows

JOHN R. KIRKPATRICK

Los Alamos Scientific Laboratory, Los Alamos, New Mexico

AND

WILLIAM F. WALKER

Department of Mechanical Engineering, Rice University, Houston, Texas 77001

Received March 2, 1971

A numerical method has been developed that is capable of describing turbulent, compressible, subsonic separated jet flow fields. The method uses a modification of the Brailovskaya two-step implicit artificial viscosity algorithm which includes an explicit artificial mass dissipation added to the continuity equation. Solutions are obtained by applying the numerical scheme to the four governing equations which describe the time-dependent, two-dimensional, turbulent, compressible flow of an ideal gas. Turbulent Reynolds stresses were described by means of the Prandtl–Görtler approximation. Starting with arbitrary initial conditions, a solution is marched forward in time until a condition satisfactorily close to steady state is achieved. Computations were performed for confined jet air flows at a March number of 0.45, wall offsets of two and four nozzle widths, and zero wall angle. The calculations were compared with experimental data and acceptable agreement was found.

INTRODUCTION

Since the development of the so-called fluid amplifier in 1960, there has been considerable effort directed toward analyzing confined jet flow fields. The operation of the bistable or wall-attachment fluidic device depends upon the Coanda effect, named for the Rumanian engineer who publicized it in 1940. This phenomenon amounts to a submerged jet of fluid being continuously deflected toward a nearby wall until reattachment occurs. A standing vortex or recirculation bubble is trapped between the jet on one side and the wall on the other side as illustrated in Fig. 1. This figure shows a wall on both sides of the jet. If the distance from the edge of the jet to each of the sidewalls (the offset) is the same, the jet can attach to either wall and is thus referred to as a bistable device. Once reattachment has occurred, the low pressure in the vortex region creates a pressure gradient across the main part of the jet that keeps the jet deflected toward the reattachment wall.

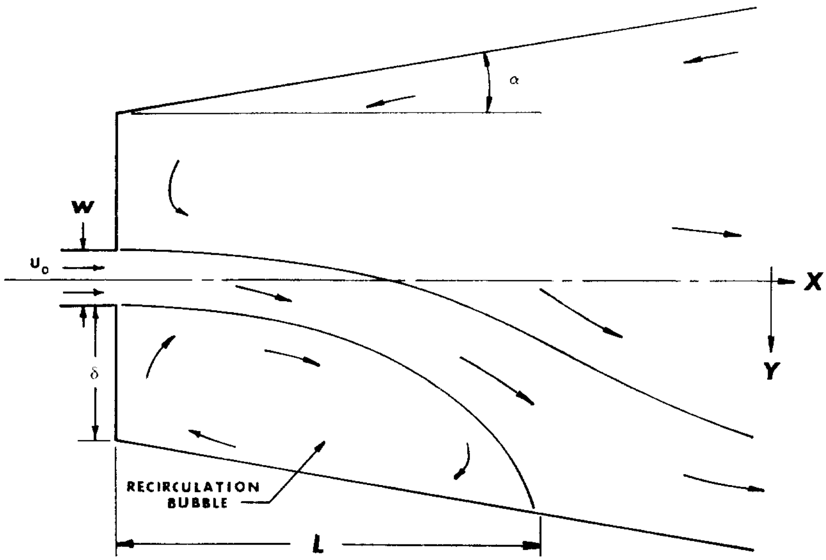

FIG. 1. Bistable fluidic device.

Most of the analytical and numerical work devoted to studying the device shown in Fig. 1 has been performed by using greatly simplified physical models. These give some of the features of the flow, usually the reattachment length and sometimes an estimate of an average recirculation bubble pressure. However, to date no numerical or analytical studies have been published which attempt to describe the complete velocity and pressure fields in a subsonic turbulent separated jet. Therefore, the primary objective of this investigation [1] was to develop a method capable of predicting the complete velocity and pressure fields in a subsonic, turbulent separated jet flow.

The first analysis of confined jet flows was performed by Bourque and Newman [2]. This has since been updated by Bourque [3] and slight variations of the basic model have been used by several other investigators [4, 5].

Each of these investigators assumed that the pressure inside the recirculation bubble was constant or else used a control volume at the reattachment point which allowed the details of the pressure variations in the flow field to be ignored. Thus, they were unable to derive any details of the pressure field. They all assumed approximate velocity profiles in the main part of the jet which resemble those which have been experimentally measured. They did not try to derive any detailed picture of the velocity profiles. The models were aimed principally at calculating the reattachment length, and were only able to obtain agreement which is at best approximate.

Zumwalt and Walker [6] suggested the method used in the present study. They recommended solving the time dependent equations of motion using an arbitrary set of initial conditions and carrying the calculations forward in time until the results converged to a steady state. The idea was apparently originated by Crocco [7]. The work which most closely parallels the present study is that of Walker *et al.* [8] who developed a numerical solution for a supersonic, turbulent free jet. However, because of the fundamental mathematical differences between subsonic and supersonic flows, the method of solution used in this study is significantly different from that reported in [8]. Roache [9], Goodrich [10], and Brailovskaya [11] all solved backstep problems which are related to the confined jet problem. All three authors studied laminar phenomena and all used the method of calculating a steady state from the time dependent equations. Roache used an explicit, one-sided "weather differencing" type of finite differencing whose details were presented by Kurzrock [12]. The origin of "weather" or "upwind" or "donor cell" differencing is attributed by Richtmeyer and Morton [13] to Lelevier. Walker and Goodrich both used the Rusanov [14] explicit artificial viscosity method and Brailovskaya used a two-step explicit (forward difference in time) method.

As noted above, the present research effort was concentrated on development of a numerical computation scheme which describes the pressure and velocity fields for the two-dimensional, subsonic, turbulent reattached jet. The method finally adopted was a modification of the two-step implicit artificial dissipation algorithm demonstrated by Brailovskaya. Calculation involves starting from a somewhat arbitrary initial condition and solving the time dependent form of the equations of motion. The time dependent solution is carried forward in time until it reaches steady state asymptotically. This steady flow is then declared the desired solution, a solution which gives the two components of velocity, as well as the pressure, as desired answers. Two cases were run to completion. The results are compared with both published experimental data taken from similar geometries and with experimental data taken at Rice University for which one of the above cases provided numerical simulation.

For this study, the working fluid was assumed to be an ideal gas with constant specific heats and with $\gamma = 1.4$. It was further assumed that the Reynolds number was sufficiently high so that the only viscous effects of importance were those due to turbulent momentum exchange, the turbulent Reynolds stresses. The Mach number in the numerical calculations was set at 0.45, a value for which some experimental data exists and for which additional usable data could be obtained with equipment available to the authors.

Governing Equations

As mentioned above, for the physical problems of interest in this investigation, molecular transport effects may be neglected in comparison with turbulent transport phenomenon. Therefore, in order to determine a mathematical description of the two-dimensional, turbulent mixing process, it is necessary to alter the inviscid hydrodynamic equations so as to include turbulence effects. The inviscid equations, which represent the conservation of mass, momentum, and energy, can be written in general conservation form, as [8]

$$\partial f/\partial t + \partial F/\partial x + \partial G/\partial y = 0, \tag{1}$$

where f, F, and G are four-component, column matrix vectors given by

$$f = \begin{bmatrix} \rho \\ \rho u \\ \rho v \\ e \end{bmatrix}; \quad F = \begin{bmatrix} \rho u \\ p + \rho u^2 \\ \rho uv \\ (e+p)u \end{bmatrix}; \quad G = \begin{bmatrix} \rho v \\ \rho uv \\ p + \rho v^2 \\ (e+p)v \end{bmatrix}, \tag{2}$$

where

$$e = \frac{p}{\gamma - 1} + \rho \frac{(u^2 + v^2)}{2}.$$

The top row in (2) corresponds to the continuity equation; the second and third rows to the x and y-momentum equations, respectively; and the bottom row to the energy equation.

For a turbulence analysis, the dependent variables are assumed to represent instantaneous values at a point. Each instantaneous value is defined, in the usual manner, as the sum of a temporal mean and a fluctuating component.

$$\begin{aligned} &u = \bar{u} + u'; \qquad v = \bar{v} + v'; \qquad p = \bar{p} + p'; \\ &\rho = \bar{\rho} + \rho'; \qquad \rho u = \overline{(\rho u)} + (\rho u)'; \qquad \rho v = \overline{(\rho v)} + (\rho v)'; \\ &e = \bar{e} + e'. \end{aligned} \tag{3}$$

The bar denotes the time average and the prime denotes the fluctuating component. The representation of (ρu) and (ρv) as fluid properties in (3) was suggested by Van Driest [15]. The fluid energy e has also been represented in this manner.

The equations which describe the general, two-dimensional, turbulent mixing process are obtained by applying the usual methods of turbulence analysis. The resulting expressions in terms of time-average quantities are:

Continuity:

$$\frac{\partial \bar{\rho}}{\partial t} + \frac{\partial \overline{(\rho u)}}{\partial x} + \frac{\partial \overline{(\rho v)}}{\partial y} = 0. \tag{4}$$

x-Momentum:

$$\frac{\partial(\overline{\rho u})}{\partial t} + \frac{\partial}{\partial x}\,[\bar{p} + \overline{\rho u}\,\bar{u} + \overline{(\rho u)'u'}] + \frac{\partial}{\partial y}\,[\overline{\rho u}\,\bar{v} + \overline{(\rho u)'v'}] = 0. \tag{5}$$

y-Momentum:

$$\frac{\partial(\overline{\rho v})}{\partial t} + \frac{\partial}{\partial x}\,[\overline{\rho v}\,\bar{u} + \overline{(\rho v)\,'u'}] + \frac{\partial}{\partial y}\,[\bar{p} + \overline{\rho v}\,\bar{v} + \overline{(\rho v)\,'v'}] = 0. \tag{6}$$

Energy:

$$\frac{\partial \bar{e}}{\partial t} + \frac{\partial}{\partial x}\{(\bar{e} + \bar{p})\bar{u} + \tfrac{1}{2}\,[\bar{u}\overline{(\rho u)\,'u'} + \bar{v}\overline{(\rho u)\,'v'}]\}$$

$$+ \frac{\partial}{\partial y}\{(\bar{e} + \bar{p})\bar{v} + \tfrac{1}{2}\,[\bar{u}\overline{(\rho v)\,'u'} + \bar{v}\overline{(\rho v)\,'v'}]\} = 0, \tag{7}$$

where

$$\bar{e} = \frac{\bar{p}}{\gamma - 1} + \frac{\overline{\rho u}\,\bar{u} + \overline{(\rho u)'u'} + (\overline{\rho v})\bar{v} + \overline{(\rho v)'v'}}{2}. \tag{8}$$

Equation (7) was obtained under the assumptions that third-order fluctuating terms are small, and that inequalities (9) and (10) are valid.

$$\overline{u^2} \gg \overline{u'^2}, \bar{u}\,\bar{v} \gg \overline{u'v'},\ \overline{v^2} \gg \overline{v'^2}, \tag{9}$$

$$\bar{p}\,\bar{u} \gg \overline{p'u'}, \bar{p}\,\bar{v} \gg \overline{p'v'}. \tag{10}$$

With regard to inequality (10), Park [16] concluded that for flows free of shock discontinuities, perturbations in pressure may be neglected for Mach numbers less than five. Since only subsonic jet flows were considered in this investigation, the assumption of negligible pressure fluctuations was adopted.

The products of the momentum and velocity flucutuating terms appearing in (5)–(7) may be interpreted as representing the rate of transfer of momentum across a surface due to turbulent fluctuations. For the turbulent stresses obtained in these equations, the matrix which defines the turbulent stress tensor (Reynolds stress tensor) is

$$\begin{pmatrix} \tau_{xx} & \tau_{xy} \\ \tau_{yx} & \tau_{yy} \end{pmatrix} = -\begin{pmatrix} \overline{(\rho u)\,'u'} & \overline{(\rho u)\,'v'} \\ \overline{(\rho v)\,'u'} & \overline{(\rho v)\,'v'} \end{pmatrix}. \tag{11}$$

To date, there is no known universal theoretical model for the turbulent Reynolds stresses. These are usually handled by semi-empirical theories which are justified to some extent by physical reasoning and by the fact that they sometimes produce results consistent with experiment. The particular model used depends on the problem to be solved, although occasionally more than one model may be used with varying success.

For turbulent jet mixing situations similar to those of interest here, the form of the Reynolds stress used is analogous to that of the ordinary Newton's law of viscosity used in laminar, viscous flows. This, following a suggestion of Boussinesq [17], involves using an expression of the form

$$\tau_{ij} = \rho\epsilon(\partial\bar{u}_i/\partial x_j), \tag{12}$$

where ϵ is the turbulent eddy viscosity. The required expression for ϵ was developed for a free jet, i.e., one which is not curved, encounters no significant pressure gradient in the streamwise or transverse directions, and is removed from any wall that will inhibit turbulent mixing. From the Prandtl–Gortler theory [8], the resulting expression for ϵ is

$$\epsilon = u_a x/2\sigma^2, \tag{13}$$

where u_a is the maximum value of the x-component of velocity at the plane in question, x is the distance from the plane to the point at which mixing began, and σ is the jet spread parameter that arises from an error function velocity profile.

In order to adapt Eq. (13), and thereby the Reynolds stresses, to the case of a reattaching jet, values of σ were varied in different regions of the flow. According to the conclusions of Mueller and Olson [18], the spread parameter should be different in each of the following three regions: (i) upsream from reattachment between the jet centerline (in this study assumed to be the line of maximum values of u) and the wall to which flow is not attached, (ii) upstream from reattachment between the jet centerline and the wall to which flow is attached, and (iii) downstream from reattachment. The appropriate values for σ for a Mach number of approximately 0.5 according to Mueller and Olson are 8.0, 10.0, and 22.0, respectively.

Upon substituting Eqs. (12) and (13) into (11), the relationship for the Reynolds stress tensor becomes

$$\begin{pmatrix} \tau_{xx} & \tau_{xy} \\ \tau_{yx} & \tau_{yy} \end{pmatrix} = -\zeta \begin{pmatrix} \dfrac{\partial\bar{u}}{\partial x} & \dfrac{\partial\bar{u}}{\partial y} \\ \dfrac{\partial\bar{v}}{\partial x} & \dfrac{\partial\bar{v}}{\partial y} \end{pmatrix}, \tag{14}$$

where

$$\zeta = u_a x/2\sigma^2.$$

The expressions for f, F, and G, including the relationships for the turbulent stresses, are therefore

$$f = \begin{bmatrix} \bar{\rho} \\ \overline{\rho u} \\ \overline{\rho v} \\ \bar{e} \end{bmatrix}; \qquad F = \begin{bmatrix} \overline{\rho u} \\ \bar{p} + \overline{\rho u}\,\bar{u} - \zeta \dfrac{\partial \bar{u}}{\partial x} \\ \overline{\rho v}\,\bar{u} - \zeta \dfrac{\partial \bar{v}}{\partial x} \\ (\bar{e} + \bar{p})\bar{v} - \dfrac{\zeta}{2}\left(\bar{u}\dfrac{\partial \bar{u}}{\partial x} + \bar{v}\dfrac{\partial \bar{u}}{\partial y}\right) \end{bmatrix}; \tag{15}$$

$$G = \begin{bmatrix} \overline{\rho v} \\ \overline{\rho u}\,\bar{v} - \zeta \dfrac{\partial \bar{u}}{\partial y} \\ \bar{p} + \overline{\rho v}\,\bar{v} - \zeta \dfrac{\partial \bar{v}}{\partial y} \\ (\bar{e} + \bar{p})\bar{v} - \dfrac{\zeta}{2}\left(\bar{u}\dfrac{\partial \bar{v}}{\partial x} + \bar{v}\dfrac{\partial \bar{v}}{\partial y}\right) \end{bmatrix};$$

where

$$\bar{p} = (\gamma - 1)\left\{\bar{e} - \tfrac{1}{2}\left[\overline{\rho u}\,\bar{u} + \overline{\rho v}\,\bar{v} - \zeta\left(\frac{\partial \bar{u}}{\partial x} + \frac{\partial \bar{v}}{\partial y}\right)\right]\right\}.$$

Equations (1) and (15) describe the two dimensional time dependent turbulent mixing process of interest. As stated earlier, the governing equations are written for the case of an ideal gas with constant specific heats. Each of the time average quantities appearing in Eq. (15) has certain dimensions associated with it. The governing equations may be rendered nondimensional rather easily with respect to conditions in the upstream jet. Letting subscript "J" denote conditions in the reference plane, and the absence of an overbar denote dimensionless time average quantities, the dimensionless dependent and independent variables are seen to be

$$p = \bar{p}/p_J, \quad \rho = \bar{\rho}/\rho_J, \quad u = \bar{u}\Big/\left[\frac{p_J}{\rho_J}\right]^{1/2}, \quad v = \bar{v}\Big/\left[\frac{p_J}{\rho_J}\right]^{1/2}$$

$$e = \bar{e}/p_J, \quad t_{ND} = \frac{t}{W}\left[\frac{p_J}{\rho_J}\right], \quad x_{ND} = \frac{x}{W}, \quad y_{ND} = \frac{y}{W}$$

Using these equations, one may show that this nondimensionalizing procedure was adopted in order to allow the governing equations to take the same form in both the dimensional and nondimensional cases.

Boundary and Initial Conditions

At the solid walls, three boundary conditions suffice. The first two conditions are that the velocity components normal and tangential to the wall should be zero. The third condition arises from reduction of the equation of momentum normal to a wall using the first two conditions. The normal momentum equation is

$$\frac{\partial \rho u_n}{\partial t} + \frac{\partial}{\partial x_t}(\rho u_n u_t) + \frac{\partial}{\partial x_n}(\rho u_n u_n) + \frac{\partial p}{\partial x_n} = \frac{\partial}{\partial x_t}\left(\zeta \frac{\partial u_n}{\partial x_t}\right) + \frac{\partial}{\partial x_n}\left(\zeta \frac{\partial u_n}{\partial x_n}\right),$$

where subscript "t" represents components tangential to the wall and subscript "n" represents components normal to the wall. Applying the first two boundary conditions, the normal momentum equation reduces to the third boundary condition

$$\frac{\partial p}{\partial x_n} = \frac{\partial}{\partial x_n}\left(\zeta \frac{\partial u_n}{\partial x_n}\right).$$

As noted earlier, laminar viscous stresses have been neglected. This obviously is in error in the immediate neighborhood of a wall. However, boundary layer theory indicates that the boundary layer thickness will be small compared with the cavity width [5]. Thus the influence of the viscous behavior of the flow near a wall should be negligible on the cavity flowfield. Of far more significance with respect to the flow-field is the boundary condition that $u_n = 0$ at the wall.

At the boundary represented by the last plane of points as the flow exits from the computational mesh, the boundary condition used was $(\partial f/\partial x) = 0$, for f as given by (15). This condition may seem unnecessarily stringent for a boundary which is not "at infinity". As a check, the conditions $(\partial^2 f/\partial x^2) = 0$ and $(\partial^3 f/\partial x^3) = 0$ were also investigated and it was found that neither convergence nor stability considerations were significantly improved.

The technique of calculating a steady state from the time dependent equations allows one to choose initial conditions which are quite arbitrary. A popular concept for initial conditions in separated flow problems is the slip line, a condition in which a line is imagined on one side of which the flow is uniform with some arbitrary velocity. On the other side of the line, the flow is uniform with a different velocity, often zero. In the present study, the initial conditions used assumed a jet which bent toward one of the walls and intercepted it at the plane of the downstream continuation. An exponential velocity profile was assumed initially.

In experiments, Levin and Manion [4] found that if the sidewall was at least twice as long as the reattachment distance, then the reattachment distance would be unaffected by the presence of any additional length of wall. This idea was adopted in the present investigation, and therefore, the calculation mesh was extended so that it was at least twice as long in the x-direction as the reattachment length given by the data of Levin and Manion.

Having the initial jet strike the wall at the exit rather than at the presumed reattachment point was a check on the ability of the numerical method to predict correct reattachment distances.

Numerical Method

The method of Brailovskaya [11] was used for the calculation of the two momentum equations and the energy equation. Unfortunately, adequate stability could not be obtained with the continuity equation using only Brailovskay's original algorithm. An additional explicit artificial mass diffusion adapted from Rusanov's method [14] was therefore added. For a system of equations of the form given by (1), Brailovskaya's method proceeds as follows. First, for time step n ($t = \sum_1^n \Delta t$), all the quantities necessary to determine the terms F and G are calculated. This includes p, u, v, ϵ, and Δt. Values of ρ, ρu, ρv, and e are already available either from previous calculations or as initial conditions. Next, a provisional time step is calculated from the equation

$$f_{j,k}^{p} = f_{j,k}^{n} - \Delta t \left[\frac{\partial F}{\partial x} + \frac{\partial G}{\partial y}\right]_{j,k}^{n}. \tag{16}$$

Values of the variables represented by f should be calculated for all points in the finite difference mesh at this provisional time. However, the values of flow variables on the boundaries should not be calculated using the boundary conditions, but rather they should be the same values as those already found for time step n. This is necessary because the two step nature of the Brailovskaya method tends to propagate oscillating pressure waves from the boundaries.

Values of the density at the provisional time step are calculated by a modified method which will be explained below. Next, a new provisional set of the variables necessary to determine F and G are calculated. In the present study, the eddy viscosity and the time step were not recalculated. However, pressure and velocity components everywhere except at the boundaries were recalculated. Next, one calculates time plane $n + 1$ via the equation

$$f_{j,k}^{n+1} = f_{j,k}^{n} - \Delta t \left[\frac{\partial F}{\partial x} + \frac{\partial G}{\partial x}\right]_{j,k}^{p}. \tag{17}$$

For the continuity equation, an explicit artificial mass diffusion from a modification of the method of Rusanov [14] has been added. The equations for calculating ρ are

$$\begin{aligned} \rho_{j,k}^{p} &= \rho_{j,k}^{n} - \Delta t \left[\frac{\partial F}{\partial x} + \frac{\partial G}{\partial y} - A\left(\frac{\partial^2 \rho}{\partial x^2} + \frac{\partial^2 \rho}{\partial y^2}\right)\right]_{j,k}^{n}, \\ \rho_{j,k}^{n+1} &= \rho_{j,k}^{n} - \Delta t \left[\frac{\partial F}{\partial x} + \frac{\partial G}{\partial y} - A\left(\frac{\partial^2 \rho}{\partial x^2} + \frac{\partial^2 \rho}{\partial y^2}\right)\right]_{j,k}^{p}, \end{aligned} \tag{18}$$

where

$$A(x, y, t) = \frac{\omega}{2}(\sqrt{u^2 + v^2} + a)\frac{\Delta x \Delta y}{(\Delta x^2 + \Delta y^2)^{1/2}}.$$

The term ω is a variable damping parameter. In a normal Rusanov algorithm calculation the value of ω must be chosen such that the inequality

$$\Delta t\,(w + c)_{\max}^{n} \sqrt{\frac{1}{\Delta x^2} + \frac{1}{\Delta y^2}} \equiv \bar{\sigma}_0{}^n \leqslant \omega \leqslant \frac{1}{\bar{\sigma}_0{}^n} \tag{19}$$

is satisfied [8]. Using the Rusanov term as an additional source of stability for the continuity equation obviated the need for rigorons adherence to this criterion. The average value of ω used in this study was approximately 0.20. This value was chosen by experimenting numerically to determine the minimum value which would control density oscillations. It is interesting to note that Brailovskaya [19] solved a problem in laminar, supersonic, recirculating wake flow and also found it necessary to add a term to the continuity equation. The added term, corresponding to A in [1] and the present study, was of the form constant $h^2 w$, where w is the modulus of the velocity vector.

Space derivatives were approximated in the usual manner. For two general dependent variables q and r, the following finite difference relations were employed:

$$\frac{\partial q}{\partial x} \approx \frac{1}{2\Delta x}(q_{j+1,k} - q_{j-1,k}),$$

$$\frac{\partial}{\partial x}\left(q\frac{\partial r}{\partial x}\right) \approx \frac{1}{2(\Delta x)^2}[(q_{j+1,k} + q_{j,k})(r_{j+1,k} - r_{j,k}) - (q_{j,k} + q_{j-1,k})(r_{j,k} - r_{j-1,k})],$$

$$\frac{\partial}{\partial x}\left(q\frac{\partial r}{\partial y}\right) \approx \frac{1}{4\Delta x \Delta y}[q_{j+1,k}(r_{j+1,k+1} - r_{j+1,k-1}) - q_{j-1,k}(r_{j-1,k+1} - r_{j-1,k-1})],$$

$$\frac{\partial^2 q}{\partial x^2} \approx \frac{1}{(\Delta x)^2}(q_{j+1,k} - 2q_{j,k} + q_{j-1,k}).$$

Other difference approximations required may be inferred from the preceding relationships.

For the governing system of equations and the difference algorithm suggested by Brailovskaya, the stability criterion yields

$$\Delta t \leqslant \min\left(\frac{h}{|u| + |v| + a\sqrt{2}}, \frac{h^2 \rho}{4 \zeta}\right), \tag{20}$$

where h is a geometric parameter that is functionally related to the mesh spacings. In practice, the first term was always dominant. As noted earlier, the Brailovskaya technique did not provide completely stable computations for the problems of interest here, i.e., a subsonic turbulent separated jet flow. Therefore, a Rusanov type artificial dissipation was added to the continuity equation. As one would suspect, the computational stability requirements were thereby altered. Numerical experimentation revealed that the first term of (20) could still be used for the combined difference approximations of Brailovskaya and Rusanov if h was expressed as

$$h = 0.7[(\Delta x)^2 + (\Delta y)^2]^{1/2} g_1(N) + \frac{g_2(N)}{\left[\dfrac{(\Delta x)^2 + (\Delta y)^2}{(\Delta x)^2 (\Delta y)^2}\right]^{1/2}}, \tag{21}$$

where

$$g_1(N) = N/1000, \qquad g_2(N) = 1 - N/1000; \qquad N < 1000,$$
$$g_1(N) = 1.0, \qquad g_2(N) = 0, \qquad N > 1000,$$

and N is the number of time steps which have been calculated. In the laminar supersonic wake problem solved by Brailovskaya [19], h was expressed as $h = \min(\Delta x, \Delta y)$.

The form of h given in (21) is a strictly empirical linear combination of two different reference distances. The first term contains a straightforward Pythagorean addition of the two sides of a mesh square. The second contains a distance which appeared in Rusanov's [14] stability criterion and also in the criterion for the Lax–Wendroff method [13].

RESULTS

Two cases were calculated in sufficient detail to illustrate the validity of the numerical scheme. Both cases were for a symmetrical confined jet device similar to that depicted in Fig. 1. A turbulent air jet with a constant jet exit Mach number of 0.45 was assumed to separate at the jet exit ($x = 0$) and flow into a cavity whose walls were parallel to the x axis (zero wall angle). The first case considered an offset of two nozzle widths (2 W) and the second an offset of four nozzle widths (4 W). Because of the two dimensional nature of the governing equations, both cases were for an infinite aspect ratio. The 2 W offset problem had a field 13 W long with a difference mesh spacing of $\Delta y/\Delta x = 1/2$. The 4 W offset case, on the other hand, had a field 20 W long with $\Delta y/\Delta x = 1/2$.

The primary purpose of the $\delta = 2\ W$ problem was to establish the convergence and stability of the computational scheme. Computations were halted after 1850 time steps, at which time the changes in pressure were less than 0.3 % in 250 time steps. This case, therefore, demonstrated that stable computations were possible and that convergence could be achieved to as close a degree as desired. For this reason, computations for the $\delta = 4\ W$ case were halted after 1375 time steps, at which time transverse pressure fluctuations were no longer detectable and pressure changes were less than 1 % in 175 time steps.

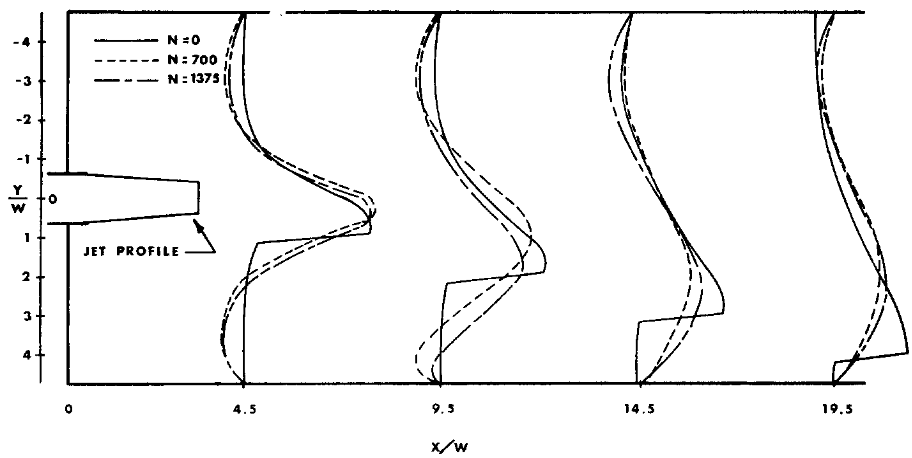

FIG. 2. Development of horizontal velocity component with time for $\delta = 4W$.

Since the results for the two cases are qualitatively similar, only the results for the 4 W case will be presented here. Figure 2 shows the development of the horizontal velocity component u, with time at selected distances along the duct. The initial velocity profile may be seen, as well as the profiles at 700 and 1375 time steps. The velocity, as well as all other properties, was held constant in the exit plane of the supply jet ($x = 0$). Although the initial conditions prescribed in the flowfield have little effect on the ultimate steady state solution, some reduction in computer time can be realized by choosing initial conditions that are near the final steady state values. For this reason, the velocity profiles shown in Fig. 2 were selected. Any other set of initial profiles would have given the same results, but the computer time required would be different.

Figure 3 shows the velocity vector diagram and Fig. 4 the isobars at time step 1375. As may be seen from the vector diagram, a recirculation region has formed in the separation bubble, thus providing qualitative agreement with what is known to occur physically. In the upper portion of the field, mass is inducted from the exit plane of the cavity and caused to flow upstream replenishing the gas that has been entrained toward the reattachment wall by the high velocity stream. This reversed flow along the upper wall is known to occur physically [20] so long as the offset is

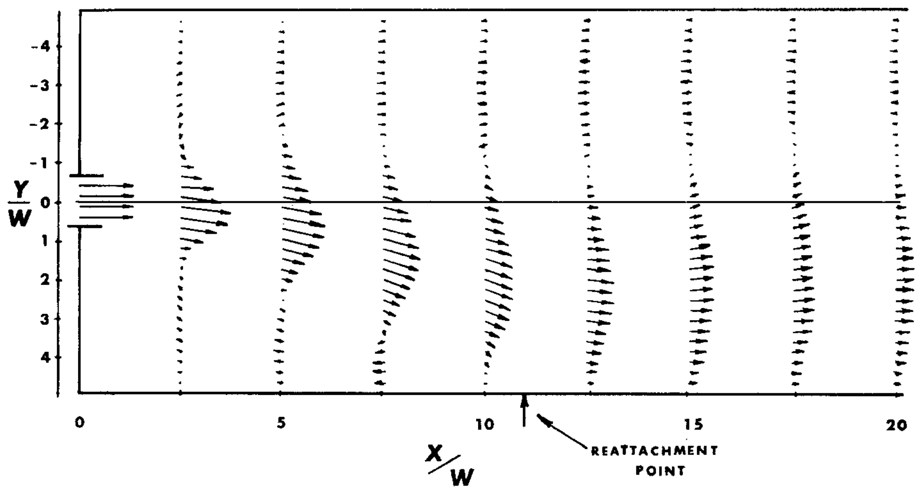

FIG. 3. Velocity vector diagram at time step 1375; $\delta = 4W$.

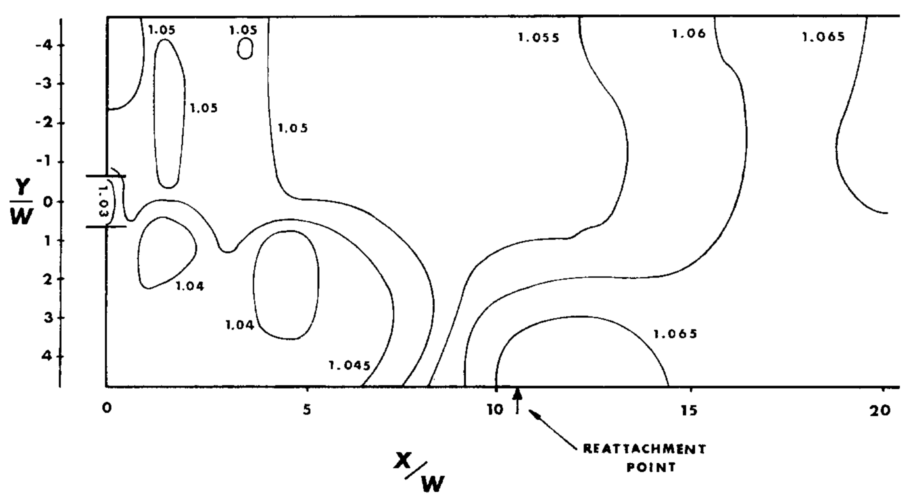

FIG. 4. Isobars at time step 1375; $\delta = 4W$.

greater than about 3 W. For offsets less than this value, a secondary attachment point with an associated recirculation bubble occurs along the upper wall, thus suppressing the induction of mass from the exit plane. It is interesting to note that for the 2 W offset case that was considered, the secondary attachement point and the associated suppression of flow along the upper wall was predicted.

The computed attachment point for the 4 W case is shown in both Figs. 3 and 4. As indicated, the flow attached to the lower wall approximately 11 W downstream from the jet exit. This compared with an attachment distance of approximately 10 W reported by Levin and Manion [4] for the case of 4 W offset and zero wall angle. However, the data of Ref. [4] were taken with only one sidewall present. Therefore, the flow was not precisely that of a confined jet since atmospheric pressure existed along the entire length of the upper boundary of the cavity. That the absence of an upper wall could in fact cause the discrepancy between the calculated reattachment length and that reported in Ref. [4] was verified by a simple modification to the 2 W offset case. For this case, the calculated reattachment distance was 9 W, whereas the distance reported in Ref. [4] was 6 W. The upper wall was removed in the computations with the result that the calculated reattachment length came into agreement with that reported in the literature.

Experimental data has been taken [21] giving pressure contours for the reattachment region in a confined jet device operating with air supplied at a Mach number of 0.45. This data was taken at offsets of 2, 4, and 6 W and wall angles of 10, 20, and 30°. Although none of these geometrical configurations is exactly the same as the ones studied in the present investigation, some comparisons can be made. For example, the approximate shape and location of the low pressure region of the calculated recirculation bubble compare favorably with the experimental data. Further, the data show that lowest pressures of about 2.5–3.5 % below ambient can be expected. Considering the pressure in the outlet plane as ambient, the minimum calculated pressures are about 3 % below this value.

In an effort to obtain additional experimental substantiation of the numerical method, the apparatus described in Ref. [21] was modified to yield wall pressure distributions. For an offset of 4 W, zero wall angle, and a jet exit Mach number of 0.45, the numerically produced and actual wall pressure distributions are shown in Fig. 5. As may be seen from the figure, relatively good agreement between numerical results and experiment has been obtained.

Figure 6 shows a comparison of the velocity profile at $x/w = 5.87$ with an experimental profile reported by Sawyer [22] at the same downstream location. The experimental data presented in Fig. 6 is for an offset of 4.62 W and only one sidewall. Thus, as in the case of the Levin and Manion results, the data of reference [22] are not entirely applicable to a confined jet flow. However, the relative comparison between the two profiles of Fig. 6 further substantiates the validity of the present method.

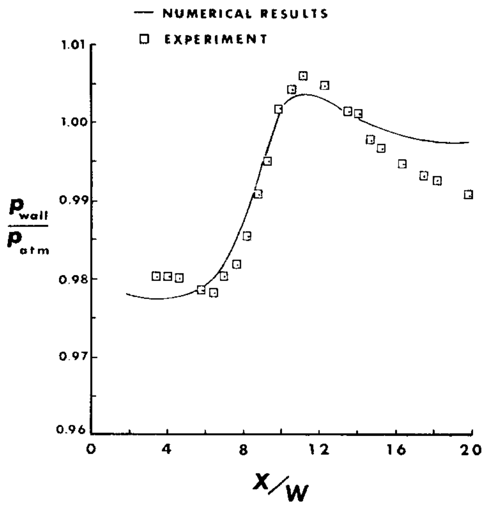

FIG. 5. Numerical and experimental wall pressure distributions; $M = 0.45$, $\delta = 4W$; $\alpha = 0$.

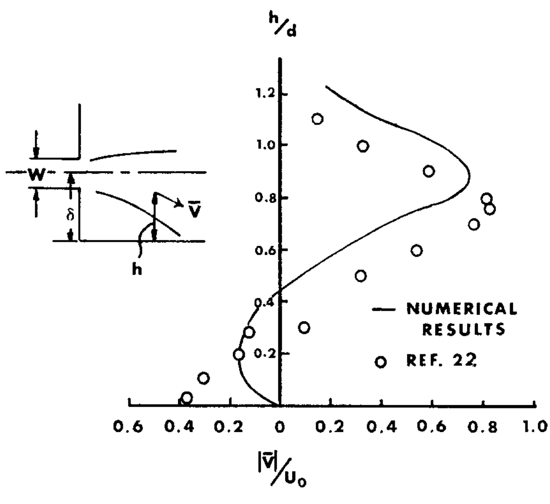

FIG. 6. Velocity profile at $x/w = 5.87$ and comparison with [22].

CONCLUSIONS

A two-step time dependent numerical method has been developed that is capable of describing steady turbulent, subsonic, separated jet flow fields. Results from the method have been compared with experimental data and favorable agreement has been found. The comparison with experiment demonstrates that even though crude, the model for the turbulent Reynolds stresses is adequate for describing the flow.

The method has not been applied to time dependent phenomena such as the switching of flow from one wall to the other. The reason for this is that the artificial dissipation inherent in the two-step time derivative is a function of the amount of of change taking place in the field. This feature would tend to distort the time dependent behavior of the flow.

References

1. J. R. Kirkpatrick, "A Numerical Study of Two-Dimensional, Turbulent, Compressible Reattached Jet Flow in Air," Ph.D. dissertation, Rice University, November, 1969.
2. C. Bourque and B. G. Newman, Reattachment of a two-dimensional incompressible jet to an adjacent flat plate, *Aero. Quart.* **5** (1960), 201–232.
3. C. Bourque, Reattachment of a two-dimensional incompressible jet to an adjacent flat plate, *Advan. Fluidics* (1967).
4. S. G. Levin and F. M. Manion, "Jet Attachment Distance as a Function of Adjacent Wall Offset and Angle," Fluid Amplification 5, Harry Diamond Laboratories, Washington, DC, Dec. 31, 1962.
5. D. I. McRee and H. L. Moses, "The Effect of Aspect Ratio and Offset on Nozzle Flow and Jet Reattachment," *Advan. Fluidics* (1967),
6. G. W. Zumwalt and W. F. Walker, "The Analysis of Submerged Jet Flow Fields by a Numerical Field Computation Method," Proceedings of the Fluid Amplification Symposium, Vol. IV, Harry Diamond Laboratories, Washington, DC, 1965.
7. L. Crocco, "A Suggestion for the Numerical Solution of the Steady Navier–Stokes Equations," AIAA Paper No. 65-1, 1965.
8. W. F. Walker, G. W. Zumwalt, and L. J. Fila, "Numerical Solution for the Interaction of a Moving Shock Wave With a Turbulent Mixing Region," *Trans. ASME Ser. E* **35** (1968), 220.
9. P. J. Roache and T. J. Mueller, "Numerical Solutions of Compressible and Incompressible Laminar Separated Flows," AIAA 68-741, 1968.
10. W. D. Goodrich, "A Numerical Solution for Problems in Laminar Gas Dynamics," Ph.D. dissertation, University of Texas, May 1969.
11. I. Brailovskaya, A difference scheme for numerical solution of two-dimensional, non-stationary Navier–Stokes Equations for a compressible gas, *Sov. Phys. Dokl.* **10** (1965), 107–110.
12. J. W. Kurzrock, "Exact Numerical Solutions of the Time-Dependent Compressible Navier-Stokes Equations," Ph.D. dissertation, Cornell University, 1966.
13. R. D. Richtmyer and K. W. Morton, *Difference Methods for Initial Value Problems*, Interscience, New York, 1967.
14. V. V. Rusanov, "The Calculation of the Interaction of Non-Stationary Shock Waves and Obstacles," National Research Council of Canada Library, Ottawa, Canada, 1962.
15. E. R. van Driest, "Turbulent Boundary Layer in Compressible Fluids," *J. Aero. Sci.* **18** (1951), 145.
16. James E. Park, "Numerical Description of Subsonic Flow in a Turbulent Compressible Boundary Layer," No. CTC-23, Union Carbide, New York, 1970.

17. J. BOUSSINESQ, "Theorie de l'Escoulement Tourbillant," Mem. Pre. par, div. Sav. No. 33, 1877.
18. T. J. MUELLER AND R. E. OLSON, "Spreading Rates of Compressible Two-Dimensional Reattaching Jets," Proceedings of the Fluid Amplification Symposium, Vol. 1, Harry Diamond Laboratories, Washington, DC, 1964.
19. I. BRAILOVSKAYA, "Flow in the Near Wake," *Sov. Phys. Dokl.* **16** (1971), 107–110.
20. JOSEPH M. KIRSHNER, "Fluid Amplifiers," McGraw-Hill, New York, 1966.
21. J. R. KIRKPATRICK, "An Experimental Study of the Pressure Contours in the Turbulent Reattachment Bubble of a Bistable Fluid Amplifier," M. S. Thesis, Rice University, 1968.
22. R. A. SAWYER, "The Flow Due to a Two-Dimensional Jet Issuing Parallel to a Blat Plate," *J. Fl. Mech.*, V. 9, 1960.